AIAA GNC Conference, Minneapolis, MN, Aug 13-16, 2012

Orion Absolute Navigation System Progress and Challenges

Greg N. Holt* and Christopher D'Souza†

NASA Johnson Space Center, 2101 NASA Parkway, Houston, TX, 77058

The absolute navigation design of NASA's Orion vehicle is described. It has undergone several iterations and modifications since its inception, and continues as a work-in-progress. This paper seeks to benchmark the current state of the design and some of the rationale and analysis behind it. There are specific challenges to address when preparing a timely and effective design for the Exploration Flight Test (EFT-1), while still looking ahead and providing software extensibility for future exploration missions. The primary onboard measurements in a Near-Earth or Mid-Earth environment consist of GPS pseudorange and deltarange, but for future explorations missions the use of star-tracker and optical navigation sources need to be considered. Discussions are presented for state size and composition, processing techniques, and consider states. A presentation is given for the processing technique using the computationally stable and robust UDU formulation with an Agee-Turner Rank-One update. This allows for computational savings when dealing with many parameters which are modeled as slowly varying Gauss-Markov processes. Preliminary analysis shows up to a 50% reduction in computation versus a more traditional formulation. Several state elements are discussed and evaluated, including position, velocity, attitude, clock bias/drift, and GPS measurement biases in addition to bias, scale factor, misalignment, and non-orthogonalities of the accelerometers and gyroscopes. Another consideration is the initialization of the EKF in various scenarios. Scenarios such as single-event upset, ground command, and cold start are discussed as are strategies for whole and partial state updates as well as covariance considerations. Strategies are given for dealing with latent measurements and high-rate propagation using multi-rate architecture. The details of the rate groups and the data flow between the elements is discussed and evaluated.

I. Introduction

The Orion spacecraft is to be NASA's next-generation Exploration vehicle for crewed missions beyond low-Earth orbit (LEO). As such, it is being designed to be capable of operating outside the comfortable confines of LEO. This introduces a variety of challenges, not least of which is the need for flexibility and robustness to a variety of environments including cislunar operations, low lunar orbit, and LEO. This paper seeks to benchmark the design of the Orion Absolute Navigation system, documenting the current state of the AbsNav system, including the challenges that have been overcome. We will first discuss the philosophy of the design and detail the architecture of the AbsNav system, then present the states in the filter, and finally present some results as related to the Exploration Flight Test 1 (EFT-1). Whereas much of the focus and effort over the past year has been directed toward EFT-1, the design is flexible enough to provide software extensibility for future exploration missions.

This paper is organized as follows: first, the overall architecture is presented including the motivation for the UDU formulation of the Extended Kalman Filter (EKF). Next, the rationale for the choice of the filter states is given. In Section 4, the recursive UDU formulation is described along with the Agee-Turner rank-

*Navigation Engineer, Flight Dynamics Division/Mission Operations, AIAA Senior Member

†Navigation Engineer, Aerosciences and Flight Mechanics Division, AIAA Senior Member

Copyright © 2012 by the American Institute of Aeronautics and Astronautics, Inc. The U.S. Government has a royalty-free license to exercise all rights under the copyright claimed herein for Governmental purposes. All other rights are reserved by the copyright owner.

one update. In Section 5, typical filter performance for a EFT-1 flight is presented along with a discussion of the implications of this performance. Finally, in Section 5, a few concluding comments are made.

II. The Architecture of the Orion Absolute Navigation System

The Orion Absolute Navigation System consists of inertial sensors and software that are used throughout the mission, from before launch to post-landing. As such, the design has to be robust to various environments and robust to various failures. The design consists of three Honeywell Orion IMUs (OIMUs), which are descendants of the Honeywell MIMU design. In addition, there are 2 GPS receivers which provide both PVT and pseudorange and deltarange measurements. Finally, there are two star trackers to provide periodic attitude updates. This is shown in Figure 1. For EFT-1 however, the Absolute Navigation System was

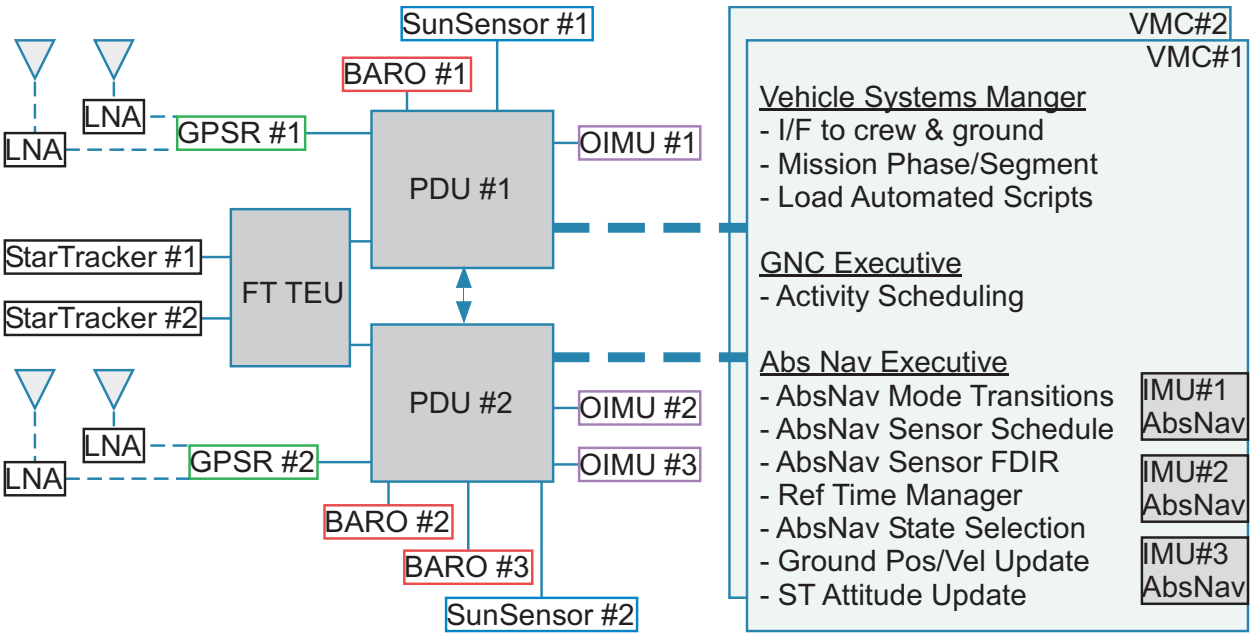

Figure 1. Orion Absolute Navigation Architecture

scaled-down to comprise 2 OIMUs and 1 GPS receiver. Because of the short duration of the flight (two orbits), there will be no star tracker carried on-board. The EFT-1 configuration is illustrated in Figure 2.

The Absolute Navigation System consists of a high-rate *Filtered Navigator* (FILTNAV), which runs at 40 Hz and a slower rate *Extended Kalman Filter* (EKF), which runs at 1 Hz. The vehicle state is propagated forward in time at 200 Hz (since the calling rate is 40 Hz, the input data is buffered) through the use of sensed ΔV and $\Delta\Theta$ data from the IMU. The output of FILTNAV is used to calculate values for use by the rest of flight software. Additionally, the propagated state (position, velocity, and attitude) is sent to the EKF, where it is the primary state propagation source. The state of the Filtered Navigator is re-synched to the estimated state of the EKF at 1 Hz intervals via a delta update.

The timing of this is rather involved and is seen in Figure 3. A few things need to be stated in order to understand the figure. First, in the Orion Flight Software (FSW) there are minor frames and major frames. There are 40 minor frames for each major frame; hence each minor frame is 0.025 seconds in duration and a major frame lasts for 1 second. Secondly, the data exchange between the major and minor frame occurs immediately prior to the beginning of the major frame. This does introduce some difficulties associated with real-time passage of data between two rate groups which need to be carefully considered.

There are several elements of the data transfer which need to be made clear. First, the 40 Hz $\Delta\theta$'s, ΔV's, State Transition Matrices (STM) ($\Phi(t_k, t_{k-1})$), and the state at time t_k ($\mathbf{X}_k^{FN}$) are transferred between FILTNAV and EKF at the major cycle boundary. At the same time, the correction to the state at time t_{k-1} ($\Delta\mathbf{X}_{k-1}$), the gravity ($\mathbf{g}$), and the gravity gradient ($\mathbf{G}$) are sent to FILTNAV. FILTNAV then uses the STM ($\Phi(t_k, t_{k-1})$) to propagate the corrections to the current time (t_k) along with it's state ($\mathbf{X}_k^{FN}$) so that

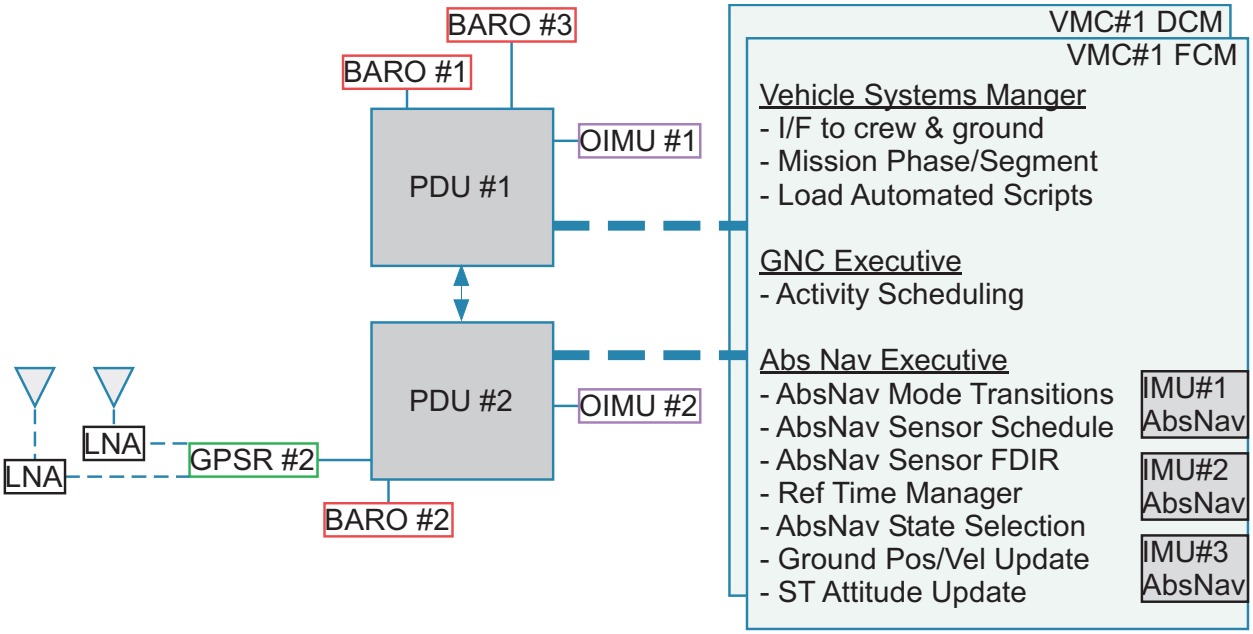

Figure 2. Orion Absolute Navigation Architecture

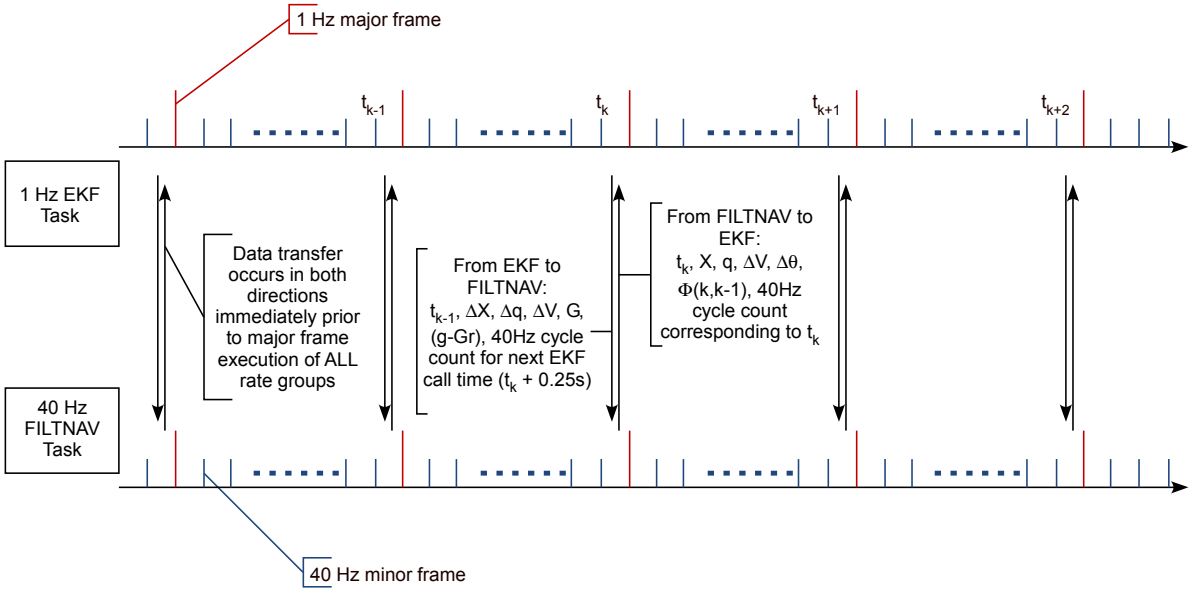

Figure 3. EKF and FILTNAV Data Exchange and Timing Diagram

$\mathbf{X}_k = \mathbf{X}_k^{FN} + \Phi(t_k, t_{k-1})\Delta\mathbf{X}_{k-1}$.

Initialization of FILTNAV and EKF occurs in a predetermined sequence to allow passing data structures to populate correctly before processing occurs. This is shown in Figure 4.

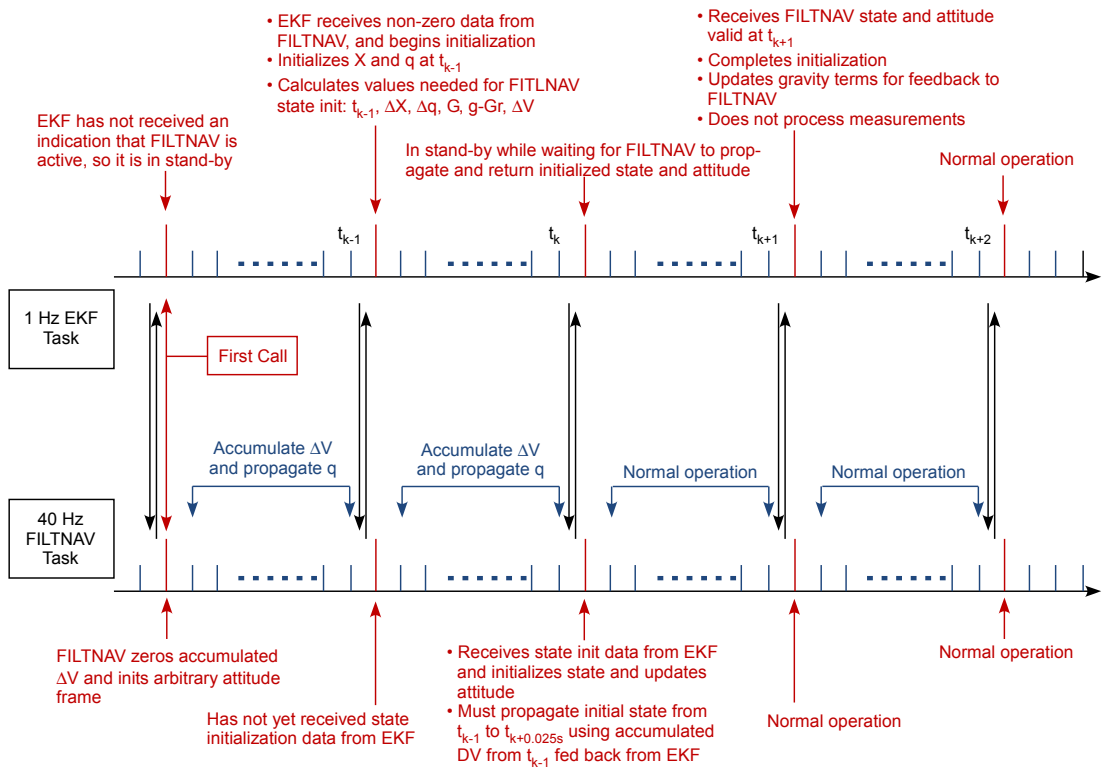

Figure 4. EKF and FILTNAV Initialization Diagram

II.A. Dynamics Modeling

In general we have the vehicle experiencing a central body gravity field with third body (Sun and Moon, if around the Earth) and non-conservative forces such as drag. Usually, the accelerometer measures these non-conservative forces, assuming they are large enough to exceed the accelerometer thresholds. With this in mind, the equations of motion are

$$\dot{\mathbf{r}} = \mathbf{v} \tag{1}$$

$$\dot{\mathbf{v}} = \mathbf{g}(\mathbf{r}) + \mathbf{a}_d + \mathbf{a}_{thirdbody} \tag{2}$$

The gravity acceleration, $\mathbf{g}(\mathbf{r})$, includes not only the two-body acceleration but the non-spherical gravity field that is usually modeled in terms of spherical harmonics.

We assume that the drag acceleration is large enough to be sensed by the accelerometers ($\mathbf{a}_s$) so that the velocity equation becomes

$$\dot{\mathbf{v}} = \mathbf{g}(\mathbf{r}) + \left(\mathbf{T}_{B_{ref}}^{I}\right)_k \mathbf{T}_B^{B_{ref}} \mathbf{T}_{\mathcal{C}}^{B} \mathbf{a}_m^{\mathcal{C}} \tag{3}$$

where $\left(\mathbf{T}_{B_{ref}}^{I}\right)_k$ is the transformation from the body frame to the inertial frame at the beginning of the cycle, $\mathbf{T}_B^{B_{ref}}$ is the transformation from the body frame during the cycle to the body frame at the beginning of the cycle, and $\mathbf{T}_{\mathcal{C}}^{B}$ is the transformation from the (IMU) case frame to the body frame.

II.B. Accelerometer Modeling

The accelerometer may be misaligned relative to the IMU reference frame. This is due to the fact that the accelerometers are not mounted orthogonal to each other and these errors are expressed in terms of small angles as:

$$\mathbf{\Xi}^a = \begin{bmatrix} 0 & \xi^a_{xy} & \xi^a_{xz} \\ \xi^a_{yx} & 0 & \xi^a_{yz} \\ \xi^a_{zx} & \xi^a_{zy} & 0 \end{bmatrix}$$

The accelerometer scale factor represents the error in conversion from raw sensor outputs (accelerometer digitizer pulses) to useful units. In general we model the scale-factor error as a first-order Markov process. It is a diagonal matrices given as

$$\mathbf{S}^a = \begin{bmatrix} s^a_x & 0 & 0 \\ 0 & s^a_y & 0 \\ 0 & 0 & s^a_z \end{bmatrix}$$

Similarly, the bias errors are modeled as as first-order Gauss-Markov processes as

$$\mathbf{b}^a = \begin{bmatrix} b^a_x \\ b^a_y \\ b^a_z \end{bmatrix}$$

So, the accelerometer measurements, $\mathbf{a}^{\mathcal{C}}_m$ are modeled as:

$$\mathbf{a}^{\mathcal{C}}_m = (\mathbf{I}_3 + \mathbf{\Xi}^a)(\mathbf{I}_3 + \mathbf{S}^a)\left(\boldsymbol{a}^{\mathcal{C}} + \mathbf{b}^a + \boldsymbol{v}_a\right) \tag{4}$$

where $\mathbf{I}_3$ is a 3×3 identity matrix, the superscript $\mathcal{C}$ indicates that this is an inertial measurement at the 'box-level' expressed in *case-frame* co-ordinates, and $\boldsymbol{a}^{\mathcal{C}}$ is the 'true' non-gravitational acceleration in the case frame. The quantity $\boldsymbol{v}_a$ is the velocity random walk, a zero-mean white sequence on acceleration that integrates into a velocity random walk, which is the 'noise' on the accelerometer output. If we assume that the errors are small, then to first-order

$$(\mathbf{I}_3 + \mathbf{\Xi}^a)(\mathbf{I} + \mathbf{S}^a) \approx \mathbf{I} + \mathbf{\Xi}^a + \mathbf{S}^a$$

So, the linear accelerometer measurements (in the case frame) are:

$$\mathbf{a}^{\mathcal{C}}_m = (\mathbf{I}_3 + \mathbf{\Xi}^a + \mathbf{S}^a)\left(\boldsymbol{a}^{\mathcal{C}} + \mathbf{b}^a + \boldsymbol{v}_a\right) \tag{5}$$

II.C. Gyro Modeling

We construct a gyro model in terms of the bias, scale factor and non-orthogonality. We assume that the $x$axis of the gyro is chosen as the reference direction with the $x - y$ plane being the reference plane; the y and z axes are not mounted perfectly orthogonal to it. Hence

$$\boldsymbol{\omega}^{\mathcal{C}}_m = (\mathbf{I}_3 + \mathbf{\Gamma} + \mathbf{S}^g)\,\boldsymbol{\omega}^{\mathcal{C}} + \mathbf{b}_g + \boldsymbol{\epsilon}_g \tag{6}$$

where

$$\mathbf{\Gamma} \triangleq \begin{bmatrix} 0 & 0 & 0 \\ \gamma_{yx} & 0 & 0 \\ \gamma_{zx} & \gamma_{zy} & 0 \end{bmatrix}, \qquad \mathbf{S}^g \triangleq \begin{bmatrix} s^g_x & 0 & 0 \\ 0 & s^g_y & 0 \\ 0 & 0 & s^g_z \end{bmatrix}, \qquad \mathbf{b}_g \triangleq \begin{bmatrix} b^g_x \\ b^g_y \\ b^g_z \end{bmatrix} \tag{7}$$

If we let $\mathbf{\Delta}^g \triangleq \mathbf{\Gamma} + \mathbf{S}^g$, we can express the actual angular velocity in terms of the measured angular velocity as

$$\boldsymbol{\omega}^{\mathcal{C}} = (\mathbf{I}_3 - \mathbf{\Delta}^g)\,\boldsymbol{\omega}^{\mathcal{C}}_m - \mathbf{b}_g - \boldsymbol{\epsilon}_g \tag{8}$$

II.D. GPS Modeling

The Orion EKF processes GPS pseudorange and deltarange measurements during its 1 Hz processing cycle. The psuedorange measurement model is formed by

$$h_{PR} = ||\mathbf{R}^I_{SV} - (\mathbf{R}^I_{ant/nav} + \mathbf{R}^{\mathbf{I}}_{\mathbf{nav}})|| + b_c + \nu_{PR} \tag{9}$$

where $\mathbf{R}^I_{SV}$ is the inertial position of the GPS satellite at the time of transmission, $\mathbf{R}^{\mathbf{I}}_{\mathbf{nav}}$ is the inertial position of the Orion navigation frame expressed in the inertial frame, $\mathbf{R}^I_{ant/nav}$ is the transformation between the receiving antenna location and the Orion navigation frame, b_c is the receiver clock bias, and ν_{PR} is the white process noise. It is assumed in this formulation, however, that the measurements are already corrected for ionospheric errors.

The Orion GPS receiver utilizes a single L1 frequency, and is thus susceptible to measurements with ionospheric delay. Options were evaluated for modeling the GPS ionosphere in different flight regimes to balance signal availability, expected delay, and filter measurement weighting. Additionally, various signal masking schema were considered. Without some sort of compensation, pseudorange errors in LEO can grow to over 80 meters. The traditional model used to compensate for ionosphere errors in a single-frequency GPS was developed by Klobuchar in 1975.[1] For LEO, we've shown this model will remove about 50% of the pseudorange error. Additionally, the residual ionosphere error signature is less like a bias and more like noise, allowing better filtering performance. The Klobuchar model is relatively simple to implement, but it does assume a "thin-shell" ionosphere concentrated at $350km$, so it can overcorrect at higher altitudes. Using the IRI2007 model as a truth reference, the residual ionosphere mis-modeling with Klobuchar compensation is demonstrated in Figure 5. Another classic compensation for ionospheric effects is to mask certain portions

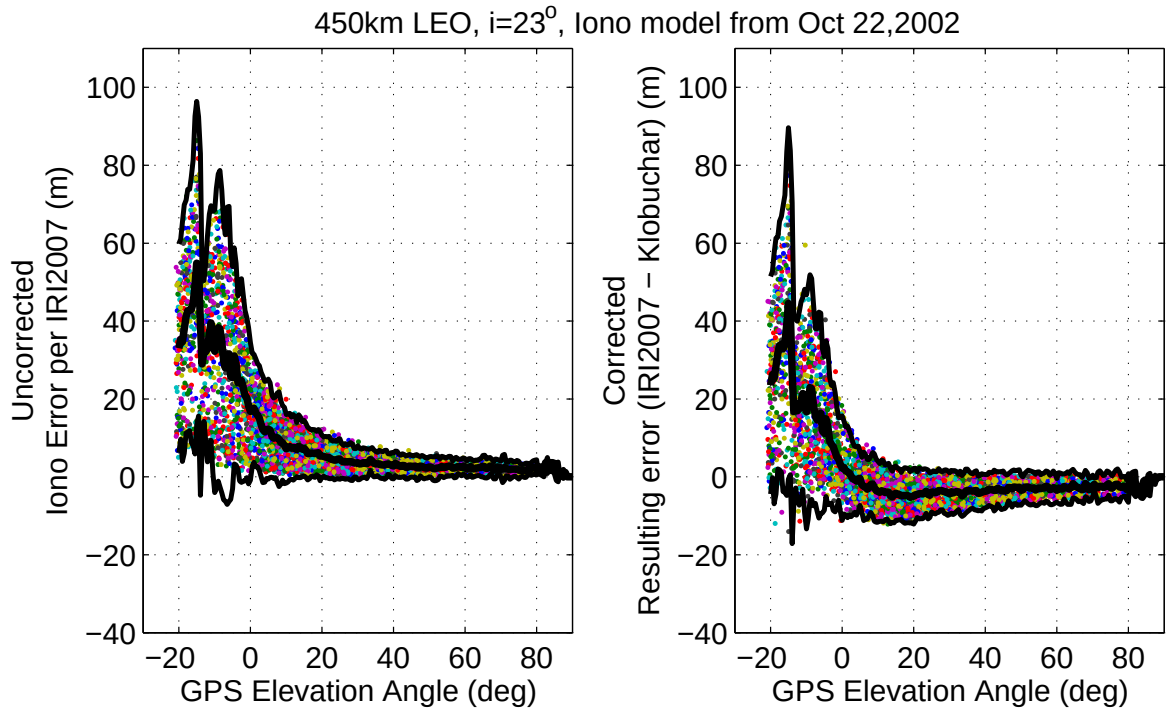

Figure 5. GPS Ionosphere Model Errors at 450km Orbit

of the observable sky that have the most severe effects. There are two implementations for this, one based on elevation angle, the other based on height above the Earth-limb. The difficulty with this method is that for higher altitudes the number of available satellites becomes restricted. From a filter standpoint, it is preferable to process all the available measurements if their error bounds can be accurately categorized. For this reason, a third option was considered that uses an analytic model based on elevation or earth limb. The proposed method was as follows, bounding the error with a weight (W) based on four analytic coefficients

$(\alpha, \beta, \gamma, \theta)$.

$$W = 5 + exp[(\frac{\ln\gamma - \ln\beta}{\alpha})(\mathrm{E} - \theta) + \ln\beta] \tag{10}$$

where below $700km$ the term (E) is the GPS satellite elevation above the local horizon in degrees and the coefficients are prescribed as (40,35,2,0). Above $700km$, (E) is the height of the GPS signal above the Earth-limb and the coefficients are prescribed as (250,205,13,350). Additionally, Klobuchar correction is applied below $450km$. While this method is appealing from a filtering standpoint, the performance improvement has not yet been judged to outweigh the additional code complexity and computational burden. The method that is currently implemented uses a modified version of the original Klobuchar model within the GPS receiver with appropriate uncertainties based on the "thin-shell" model.

II.E. The Filter States

Filter performance is affected by many factors: sensor measurement errors, data rates, tuning, and others. Foremost among these is the number and type of states that are modeled. If too many states are chosen, the filter is slow; if not enough states are modeled, the filter will perform poorly. The Orion EFT-1 Extended Kalman Filter has 11 states and 24 ECRV (Exponentially Correlated Random Variable) parameters.

The first set of 'dynamic states' are: position (3 states), velocity (3 states), attitude (3 states), clock bias and clock drift (2 states). We explicitly include the attitude as a state in order to properly model the coupling inherent in a strapdown IMU (particularly during accelerated flight). The 24 parameters are modeled as first-order Gauss-Markov processes and use a much more efficient computational algorithm for the update of the covariance matrix. It is noteworthy that the ECRV parameters for accel/gyro misalignment and nonorthogonality are only minimally observable, but are included in the filter as a means of informing the filter that the sensor parameters are time-varying; in addition, they provide an additional set of tuning parameters to obtain better performance – in the form of the time constants associated with the first-order Gauss-Markov processes and the process noise associated with each sensor parameter. Since the IMU has a 'high g / low g' switch, separate accelerometer biases for low-G and high-G are included in the filter. As well, the computational burden associated with the three additional accelerometer bias states is small because of the way Gauss-Markov states are incorporated.

So, the 24 sensor states in the filter, modeled as first-order Gauss-Markov processes, are as follows: High-g accelerometer bias (3 states), Low-g accelerometer bias (3 states), Accelerometer scale-factor (3 states), Accelerometer misalignment (6 states), Gyro bias (3 states), Gyro scale-factor (3 states), Gyro non-orthogonality (3 states).

In passing, we mention that the accelerometers are not mounted orthogonal to each other and these misalignments are modeled as a six-parameter small angle vector. The accelerometer scale factor represents the error in conversion from raw sensor outputs (accelerometer digital pulses) to useful units.

For the gyros, we assume that the x-axis of the gyro is chosen as the reference direction with the x-y plane being the reference plane, the y and z gyros not being mounted perfectly orthogonal to it. We use only three parameters to model this non-orthogonality.

All of these IMU states are estimated in the case-frame in order to avoid a mixing of time constants between the various parameters.

III. The UDU Formulation of the Orion Absolute Navigation System

The UDU formulation of the Kalman Filter has been used in aerospace engineering applications for several decades. Bierman and Thornton[2] and Bierman[3] introduced an elegant UDU formulation in order to improve the computational stability and efficiency of large navigation filters, originally used in a batch formulation. However, this formulation lent itself to sequential implementations, well-suited for platforms where both computational stability and numerical efficiency were at a premium.

Due to the fact that there are three EKF's operating on Orion, each one slaved to one IMU, and the large number of states, it was decided to use the UDU formulation of the EKF for the Orion Absolute Navigation System.

The UDU formulation has, as it's heritage, the singular value decomposition (SVD), in which any $m \times n$ matrix can be decomposed into two unitary matrices and a single diagonal matrix. For our case, we are

concerned with the decomposition of the covariance matrix, which is a real, symmetric, positive definite matrix. Such a matrix, $\mathbf{P}$, can be decomposed by means of an upper triangular, orthogonal matrix $\mathbf{U}$, and a diagonal matrix $\mathbf{D}$, containing the singular values of $\mathbf{P}$, as

$$\mathbf{P} = \mathbf{U}\mathbf{D}\mathbf{U}^T \tag{11}$$

III.A. The Time Update

The efficiency and robustness of the UDU formulation have been harnessed in the time-update of the covariance matrix. This takes on particular import because of the partitioning of the overall state into the dynamic states and the parameters modeled as first-order Gauss-Markov processes. In general, there are two techniques used to propagate the covariance in an Extended Kalman Filter. One way is to integrate the covariance matrix using the Ricatti equation, perhaps taking advantage of the symmetry and only integrating $\frac{n(n-1)}{2}$ terms. However, the most common method of propagating the covariance matrix is to use the STM; and the UDU formulation is particularly well-suited for this. This offers particular advantages in the case of the Orion Absolute Navigation Filters since the vast majority of the states (24) are first-order Gauss-Markov states; since the dynamics of these states are uncoupled, the state transition matrix is expressed analytically. Additionally, the STM for the dynamic states (the position, velocity, attitude, and GPS clock states) are computed using a first-order approximation; this is particularly appropriate in the 40 Hz rate-group. Care is taken in the computation of the state transition matrix in the 1 Hz rate-group where additional terms are incorporated.

III.A.1. The Modified Gram-Schmidt Orthogonalization

In particular, the modified Gram-Schmidt Orthogonalization, as detailed in Bierman[3] is used to update the dynamic states. The adjective *modified* serves to denote the fact that the *ordinary* Gram-Schmidt orthogonalization often results in basis vectors which are not quite orthogonal, caused by round-off errors. The *modified* Gram-Schmidt orthogonalization process obviates this difficulty by ensuring that every step in the orthogonalization process results in orthogonal basis vectors. It is functionally and mathematically equivalent to the classic Gram-Schmidt orthogonalization.

For a large number of states, most of which might be biases (or Gauss Markov processes), much of this is wasted considering the sparseness of $\mathbf{\Phi}$, the state transition matrix. The modified Gram-Schmidt algorithm uses $[1.5n_{\mathbf{x}}^3 + 0.5n_{\mathbf{x}}^2(2m_{\mathbf{x}} - 1)]$, and $[0.5n_{\mathbf{x}}^2(3n_{\mathbf{x}} + 1) + n_{\mathbf{x}}m_{\mathbf{x}}(n_{\mathbf{x}} + 1)]$ mulitplies and $[(n_{\mathbf{x}} + m_{\mathbf{x}})(n_{\mathbf{x}} - 1)]$ divides. For $n_{\mathbf{x}} = 35$ and $m_{\mathbf{x}} = 35$ (the number of states affected by process noise), we use 85,750 adds and 88,200 multiplies – quite a large number of computations.

But we can do better! We can vastly improve (reduce) on the number of computations by 'factoring' the states into 'states' and 'parameters'. This is the motivation for separating the overall states into states and (Gauss-Markov) parameters. These time-update to the parameters are handled differently. In fact, the dynamic states (position, velocity, attitude and clock states) are updated via the modified Gauss-Markov process; the time update equations are expanded so that the Agee-Turner time update is used to perform the update to the Gauss-Markov states.

III.A.2. The Agee-Turner Rank-One Time Update

We recall that most of the states are sensor first-order Gauss-Markov states. If the modified Gram-Schmidt algorithm is used without taking advantage of the fact that the sensor states are not coupled with one another, we incur wasted computations. Therefore, we take advantage of an algorithm introduced in 1972 by Agee and Turner[4] of the White Sands Proving Ground to significantly reduce the computations involved in time update of the covariance associated with the sensor states.

III.A.3. The Inclusion of Process Noise

Navigators use process noise to tune the filter. For the Orion Absolute Navigation Filter, the process noise enters covariance update via the dynamic states and the sensor parameters. For the position and velocity, the process noise enters via the velocity state; the process noise represents the uncertainty in the dynamics, chiefly via mis-modeled accelerations. Since the accelerometer measure non-inertial forces, gravity is modeled via a high-order gravity model. For the Orion Absolute Navigation filter, Earth's gravity is modeled by an

8×8 gravity field; higher-order spherical harmonics are neglected and hence are included in the velocity process noise. Additionally, since the attitude rate states are not part of the filter, the attitude process noise enters via the gyro angle random walk. Likewise, during powered flight, velocity process noise enters into the velocity channels. Of course, the sensor parameters are modeled as first-order Gauss-Markov processes and bring with them corresponding process noise parameters which are used in the tuning of the filter. The GPS clock model brings with it a clock bias and clock drift process noise which affect the GPS clock states.

The Gram-Schmidt orthogonalization assumes that the process noise is diagonal. However, this is clearly not the case. A Cholesky square-root free factorization is performed on the process noise associated with the dynamic states; once this is done the machinery associated with the UDU factorization can proceed unhindered.

III.A.4. The Computational Burden of the Time Update

So, what is the computational cost of using the UDU time update? It is observed that the UDU factorization time update, with all the above modifications, use following arithmetic operations:

$$\text{Adds}: \quad 1.5n_{\mathbf{x}}^3 + n_{\mathbf{x}}^2 m_{\mathbf{x}} + n_{\mathbf{x}}^2 n_{\mathbf{p}} - 0.5n_{\mathbf{x}}^2 + n_{\mathbf{p}} + n_{\mathbf{x}}(n_{\mathbf{p}}+1)n_{\mathbf{p}} + \sum_{k=1}^{n_{\mathbf{p}}} k^2$$

$$\text{Multiplies}: \quad 0.5n_{\mathbf{x}}^2(3n_{\mathbf{x}}+1) + n_{\mathbf{x}}m_{\mathbf{x}}(n_{\mathbf{x}}+1) + (5.5 + 5n_{\mathbf{x}} + n_{\mathbf{x}}^2)n_{\mathbf{p}} + \frac{1}{2}(2n_{\mathbf{x}}+5)n_{\mathbf{p}}^2 + \sum_{k=1}^{n_{\mathbf{p}}} k^2$$

$$\text{Divides}: \quad (n_{\mathbf{x}} + m_{\mathbf{x}})(n_{\mathbf{x}} - 1) + n_{\mathbf{p}}$$

For $n_{\mathbf{x}} = 9$, $m_{\mathbf{x}} = 9$, $n_{\mathbf{p}} = 26$, we will utilize 16,407 adds, 19,338 multiplies, and 170 divides. In contrast, if we did the MGS on all 35 states ($n_{\mathbf{x}} = 35$, $m_{\mathbf{x}} = 35$ and $n_{\mathbf{p}} = 0$), we would use 85,750 adds, 88,200 multiplies, and 34 divides. Finally, if the covariance were updated (without any consideration given to the structure of Φ from $\Phi\bar{\mathbf{P}}\Phi^T$, with $n_{\mathbf{x}} = 35$, $m_{\mathbf{x}} = 35$, we would have 84,525 adds, 85,750 multiplies and no divides[a].

III.B. The Measurement Update

For the Orion Absolute Navigation Filter, measurements are processed one-at-a-time. Both the delta-update to the state and to the covariance are accumulated at a given epoch; only after all measurements at an epoch are processed are the state and the covariance updated. This is done to preclude any dependence on the *order* of measurement processing. This is, in effect, a linear update of the states and covariance by the measurements.

With this in mind, all the measurement updates are, in effect, rank-one updates to the covariance matrix. However, since this rank one update is of the form

$$\mathbf{UDU}^T = \overline{\mathbf{U}}\left[\overline{\mathbf{D}} - \frac{1}{\alpha}\mathbf{v}\mathbf{v}^T\right]\overline{\mathbf{U}}^T$$

noting the negative sign in the above expression which does not allow the methodology of the rank-one time-update to be used for loss of numerical precision.[5] We note that, in the above equation,

$$\begin{aligned} \mathbf{v} &= \overline{\mathbf{DU}}^T\mathbf{H}^T \\ \alpha &= \mathbf{H}\overline{\mathbf{UDU}}^T\mathbf{H}^T + \mathbf{R} \end{aligned}$$

[a]For arbitrary matrices, $\mathbf{A}$ and $\mathbf{B}$ of dimension $n \times m$ and $m \times p$, respectively, the product

$$\mathbf{C} = \mathbf{AB} \tag{12}$$

results in $n(m-1)p$ adds,nmp multiplies and no divides.

and $\overline{\mathbf{U}}$ and $\overline{\mathbf{D}}$ are the *a priori* upper triangular and diagonal decomposition matrices of the covariance matrix $\overline{\mathbf{P}}$.

Whereas the details of the rank-one measurement update are somewhat obscure, the resulting numerically stable recursion avoids loss of precision involved in the differencing of two positive quantities which are of similar size.

III.B.1. The Computational Burden of the UDU Measurement Update

Thus, taking advantage of the triangularity of the $\overline{\mathbf{U}}$ matrix, for each measurement processed, the covariance update results in $1.5n_{\mathbf{x}}^2 - 0.5n_{\mathbf{x}}$ adds, $1.5n_{\mathbf{x}}^2 + 1.5n_{\mathbf{x}}$ multiplies and $3n_{\mathbf{x}} - 1$ divides.

For the normal, Joseph filter update ($\mathbf{P} = (\mathbf{I} - \mathbf{KH})\,\widehat{\mathbf{P}}\,(\mathbf{I} - \mathbf{KH})^T + \mathbf{KRK}^T$), for a scalar measurement, we find that if we use efficient methods of calculating and storing quantities,[3] we use $4.5n_{\mathbf{x}}^2 + 3.5n_{\mathbf{x}}$ adds, $4n_{\mathbf{x}}^2 + 4.5n_{\mathbf{x}}$ multiplies and 1 divide.

For the "Conventional" Kalman filter update ($\mathbf{P} = \widehat{\mathbf{P}} - \mathbf{KH}\hat{\mathbf{P}}$), for a scalar measurement, we find that[3] we use $1.5n_{\mathbf{x}}^2 + 1.5n_{\mathbf{x}}$ adds, $1.5n_{\mathbf{x}}^2 + 0.5n_{\mathbf{x}}$ multiplies and 1 divide.

Thus, for $n_{\mathbf{x}} = 35$, the covariance update due to measurement processing with the UDU factorization uses 1820 adds, 1890 divides and 104 divides compared with 5635 adds, 5058 multiplies and 1 divide for the efficient Joseph update. The "Conventional" Kalman update uses 1890 adds, 1855 multiplies, and 1 divide.

Hence there almost a factor of 2.5 improvement in the adds and multiplies using the triangular (UDU) update compared with the Joseph update. This rivals the efficiency of the "conventional" Kalman Filter update.

III.C. Consider Covariance Capability with the Orion Absolute Navigation System

'Consider' Analysis was first introduced by S. F. Schmidt of NASA Ames in the mid 1960s as a means to account for errors in both the dynamic and measurement models due to uncertain parameters.[6] The Consider Kalman Filter, also called the Schmidt-Kalman Filter, resulted from this body of work. The consider approach is especially useful when parameters have low observability. This, of course, is precisely the situation of the Orion Absolute Navigation EKF.

In it's essence, the consider parameters are not updated. In particular, the Kalman gain associated with the consider parameters, $\mathbf{p}$, is zero, *i.e.* $\mathbf{K_p} = \mathbf{0}$. However, several comments are in order:

1. When using the Schmidt-Kalman filter, the *a priori* and *a posteriori* covariance of the parameters ($\mathbf{P_{pp}}$) are the same.

2. The *a posteriori* covariance matrix of the states and the correlation between the states and the parameters are the same regardless of whether one uses the Schmidt-Kalman filter or the optimal Kalman update

The UDU formulation, while numerically stable and tight, is quite inflexible to making any changes in the framework. At first blush, it would seem that the consider analysis would not fit into the framework. However, all is not in vain. With some clever rearrangements, we can allow for a rank-one update to include consider states in the measurement update. The measurement update, expressed in terms of the consider covariance, is

$$\mathbf{P}_{opt}^{+} = \mathbf{P}_{con}^{+} - W\,(\mathbf{SK}_{opt})\,(\mathbf{SK}_{opt})^T \tag{13}$$

where $\mathbf{S}$ is an $n_{\mathbf{x}} \times n_{\mathbf{x}}$ matrix (defining $n_{\mathbf{x}} \triangleq n_{\mathbf{s}} + n_{\mathbf{p}}$, where $n_{\mathbf{x}}$ is the total number of states, $n_{\mathbf{p}}$ is the number of consider states, and $n_{\mathbf{s}}$ is the number of "non-consider" states) defined as

$$\mathbf{S} \triangleq \begin{bmatrix} \mathbf{0}_{\mathbf{n_s}\times\mathbf{n_s}} & \mathbf{0}_{\mathbf{n_s}\times\mathbf{n_p}} \\ \mathbf{0}_{\mathbf{n_p}\times\mathbf{n_s}} & \mathbf{I}_{n_{\mathbf{p}}\times n_{\mathbf{p}}} \end{bmatrix} \tag{14}$$

Since we are processing scalar measurements, we note that $W = \frac{1}{\alpha}$ is a scalar and $\mathbf{K}_{opt}$ is an $n_{\mathbf{x}} \times 1$ vector. Therefore $\mathbf{SK}_{opt}$ is an $n_{\mathbf{x}} \times 1$ vector. Therefore, solving for the consider covariance,

$$\mathbf{P}_{con}^{+} = \mathbf{P}_{opt}^{+} + W\,(\mathbf{SK}_{opt})\,(\mathbf{SK}_{opt})^T \tag{15}$$

Eq. (13) has the same form as the original rank-one update *i.e.* $\mathbf{P}^+ = \mathbf{P}^- + c\mathbf{a}\mathbf{a}^T$. With this in mind, we can use the (un-modified) rank-one update which is a backward-recursive update.[4] If, for example, all the consider parameters are in the lower part of the state-space, we can effectively reduce the computations by ending the update when the covariance of the state of the last consider parameter is updated.

Therefore, the procedure is as follows: first perform a complete rank-one measurement update with the optimal Kalman Gain ($\mathbf{K}_{opt}$) according to the *modified* rank-one update – on the full covariance matrix. Second, perform another rank-one update with $\mathbf{a} = \mathbf{S}\mathbf{K}_{opt}$ and $c = W$, according to the (un-modified) rank-one update (as in Table 1).

Therefore, since there is an additional rank-one update associated with the consider states and if no rearrangement of the consider states are performed, then there will be an additional $n_{\mathbf{x}}^2$ adds, and $n_{\mathbf{x}}^2+3n_{\mathbf{x}}+2$ multiplies, and $n_{\mathbf{x}} - 1$ divides per measurement.

The use of the 'consider state' option, if it is exercised, is likely to be used in 'consider'ing the attitude states, particularly during entry. The rationale for this is that in certain degenerate cases, when GPS satellites are reacquired after entry blackout, the attitude could be adversely affected. So, to protect for this, the 'consider' option may be exercised with respect to the attitude states.

IV. Performance of the Orion Absolute Navigation System

The performance of the Orion Absolute Navigation System is described in particular for the EFT-1 mission. This test flight consists of a low altitude orbit phase, a high altitude orbit phase, and a high energy re-entry trajectory that is designed to be somewhat representative of a beyond LEO mission.

IV.A. Position and Velocity

After implementing all the changes detailed in the previous sections, the performance of the Orion Absolute Navigation system was analyzed. A high-fidelity simulation environment, OSIRIS, was used to simulate the performance of the AbsNav system. The flight phase of most concern to the Orion navigation team for the EFT-1 mission is the terminal Earth approach, entry, descent, and landing. A simulation was performed that begins at the apogee of a high-altitude orbit and continues to descend toward Earth's atmosphere, with the resulting navigation error presented in Figure 6. In the simulation, signals from the GPS constellation gradually become visible over the first 1,000 seconds. A 100 second IMU outage is simulated around 1,900 seconds. The vehicle encounters the atmosphere at around 3,000 seconds where it experiences a measurement blackout of approximately 200 seconds due to plasma attenuation of the L-band GPS signal. The simulation terminates with parachute deploy, descent, and splashdown. Some noteworthy results seen in the figure include

1. The initial variance and navigation error is large, simulating an extended outage of GPS measurement availability as the Orion trajectory travels outside the terrestrial service volume.

2. Measurement underweighting allows for incorporation of individual GPS measurements as they become available without overconverging the filter.

3. Errors and uncertainties grow rapidly during the plasma blackout as the vehicle experiences a highly dynamic environment with no measurement updates

4. Performance returns quickly to steady-state after emergence from the plasma blackout, well in time to support parachute deploy and touchdown accuracy needs.

IV.B. Attitude

Because the Orion Absolute Navigation filter design utilizes coupled attitude states, the performance of the attitude estimate is to some extent tied to the overall capability of the filter. For this simulation, attitude states are initially assumed uncorrelated with the position and velocity after long periods of no direct attitude observability. The attitude error is shown in Figure 7. Some items of note in the figure include

1. The initial variance is large, simulating an extended period with no direct attitude observability as the Orion trajectory travels outside region of IMU-sensed acceleration with no star-tracker updates.

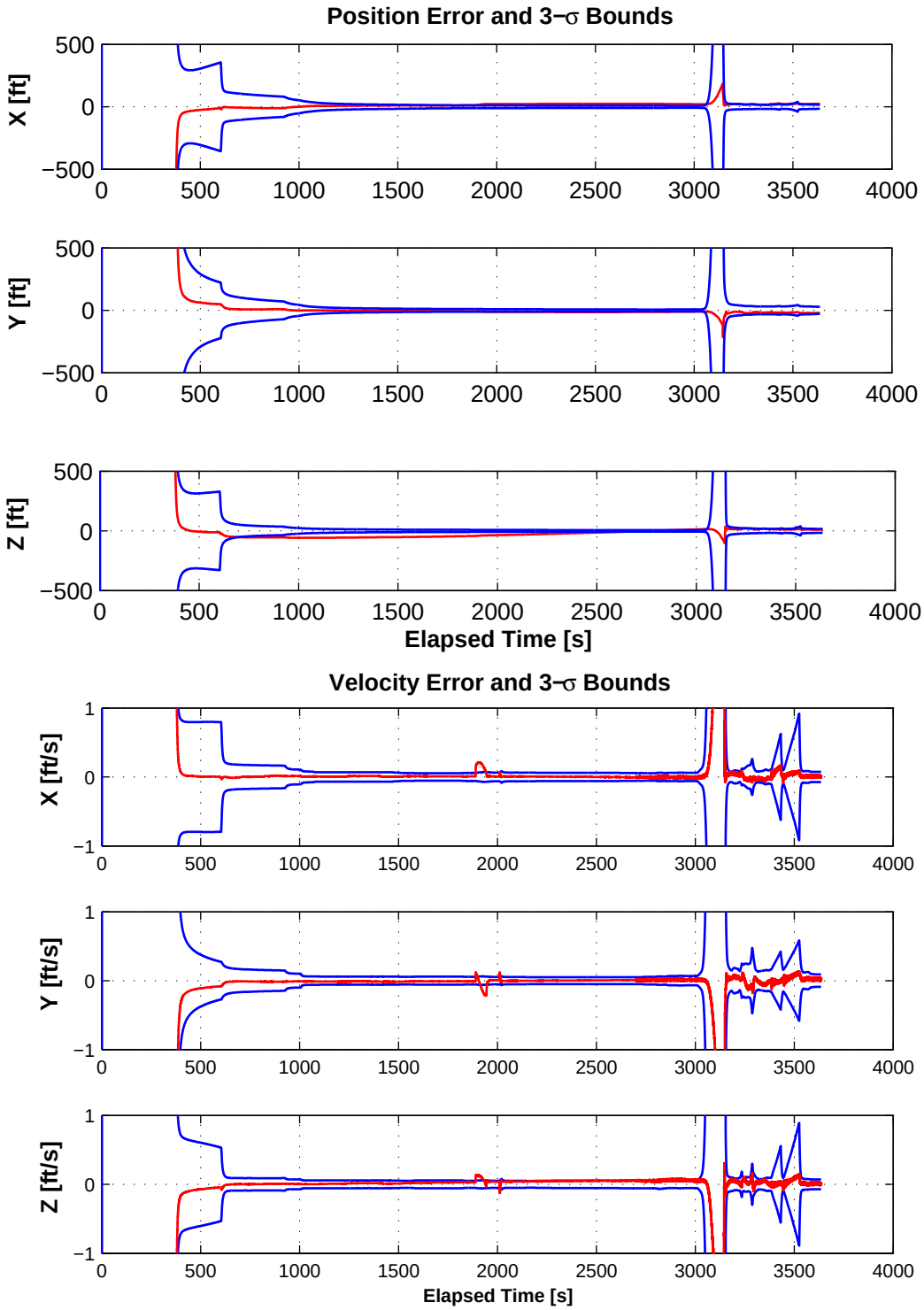

Figure 6. Nominal Position and Velocity Estimation Performance

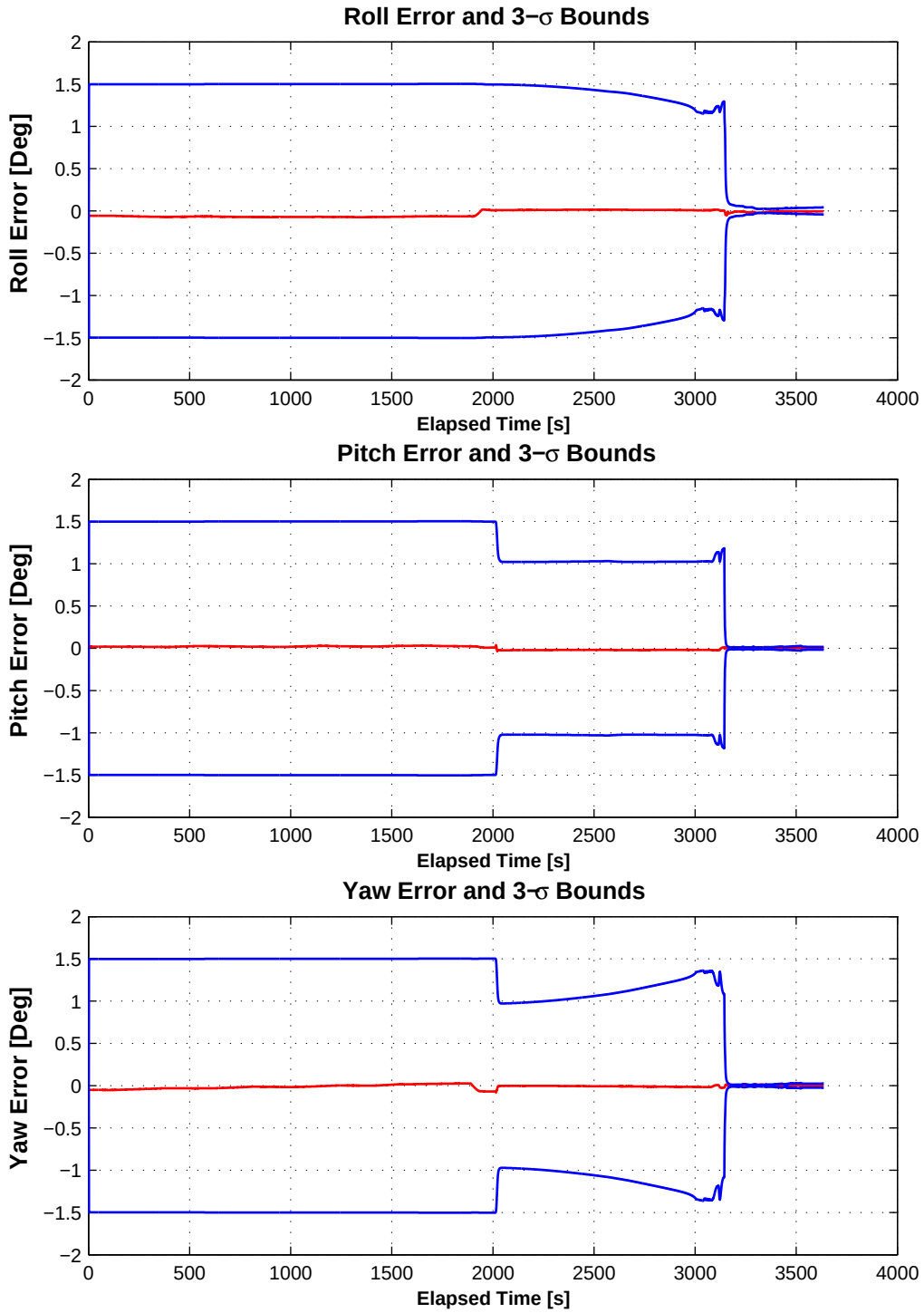

Figure 7. Attitude Estimation Performance

2. A simulated trim burn around 2,000 seconds gives brief attitude observability and the filter uncertainties reflect that improvement.

3. The full advantage of the coupled filter is realized after the plasma blackout when GPS measurements are processed in the presence of IMU-sensed accelerations. The attitude uncertainties decrease dramatically at that point.

IV.C. GPS Clock Estimates

When processing raw GPS observables, the clock bias and drift estimates play a crucial role in the performance of the filter. The clock estimates and uncertainties become especially crucial when attempting to process sparse GPS measurements after an extended measurement outage. The GPS clock error estimates are shown in Figure 8. Some items of note in the figure include

1. The initial uncertainty grows when few GPS measurements are present. As more measurements become available, the uncertainty begins to collapse.

2. With three satellites available, the drift estimate begins to converge. Once four satellites become available, the bias estimate rapidly converges.

3. The high dynamics experienced during entry stress the drift estimate as sensed accelerations are interpreted as shifts in the drift rate of the clock.

V. Recent Developments and Challenges

V.A. Cross Channel Initialization

A heightened concern amongst the Orion navigation team arises from the increased probability of multiple in-flight restarts of the EKF due to radiation hits, etc. One advantage of redundant flight computers, however, is the ability to bootstrap a restarted EKF from its counterpart on the working computer. If the event were infrequent or very low probability, then one could probably just get away with passing the position, velocity, and attitude states across a restart, zeroing out the other states, and using canned variances that are conservatively large. Doing this multiple times, however, will cause a large performance impact. For this reason, the team has decided to additionally pass all the state variances as well as the PVA correlations between the flight computers. Because this capability was added later in the design, the data size of the cross-channel bus had been fixed and great lengths had to be taken to pack the needed information into the existing space. For this reason, prior to passing, all variances were recast as single precision, all auxiliary states except GPS clock bias were recast as single precision, and the upper 9x9 triangular PVA correlation coefficients were recast as 16-bit integers scaled to 4 significant digits. This same initialization method is used for a "warm" restart (one flight computer down) or for a "cold" restart (both flight computers down). It was desired to use this same methodology for a ground state update as well, but the command interfaces were too well defined by the time the navigation team realized this need. For a ground update, then, a canned onboard covariance matrix is used, however the ground can specify an optional scale factor to apply to the matrix to better reflect the uncertainty in the update.

V.B. Measurement Underweighting

Measurement underweighting has long been standard practice in manned on-board navigation since Apollo.[7] This is used in lieu of a second-order measurement update which is used in the so-called second-order EKF, which is more computationally expensive. Underweighting is needed when accurate measurements (such as GPS) are introduced at a time when the *a priori* covariance (particularly of the position and velocity states) matrix is large. In the case of GPS measurements, the update to the position and velocity states would result in the covariance matrix associated with these states 'clamping' down too fast. The underweighting factor slows down the rate at which the covariance decreases, introducing by essentially approximating the second-order terms of the Taylor series which are not explicitly included in the EKF. Underweighting is typically implemented during the Kalman Gain calculation by

$$\mathbf{K} = \mathbf{P}\mathbf{H}^T((\alpha+1)\mathbf{H}\mathbf{P}\mathbf{H}^T + R)^{-1}$$

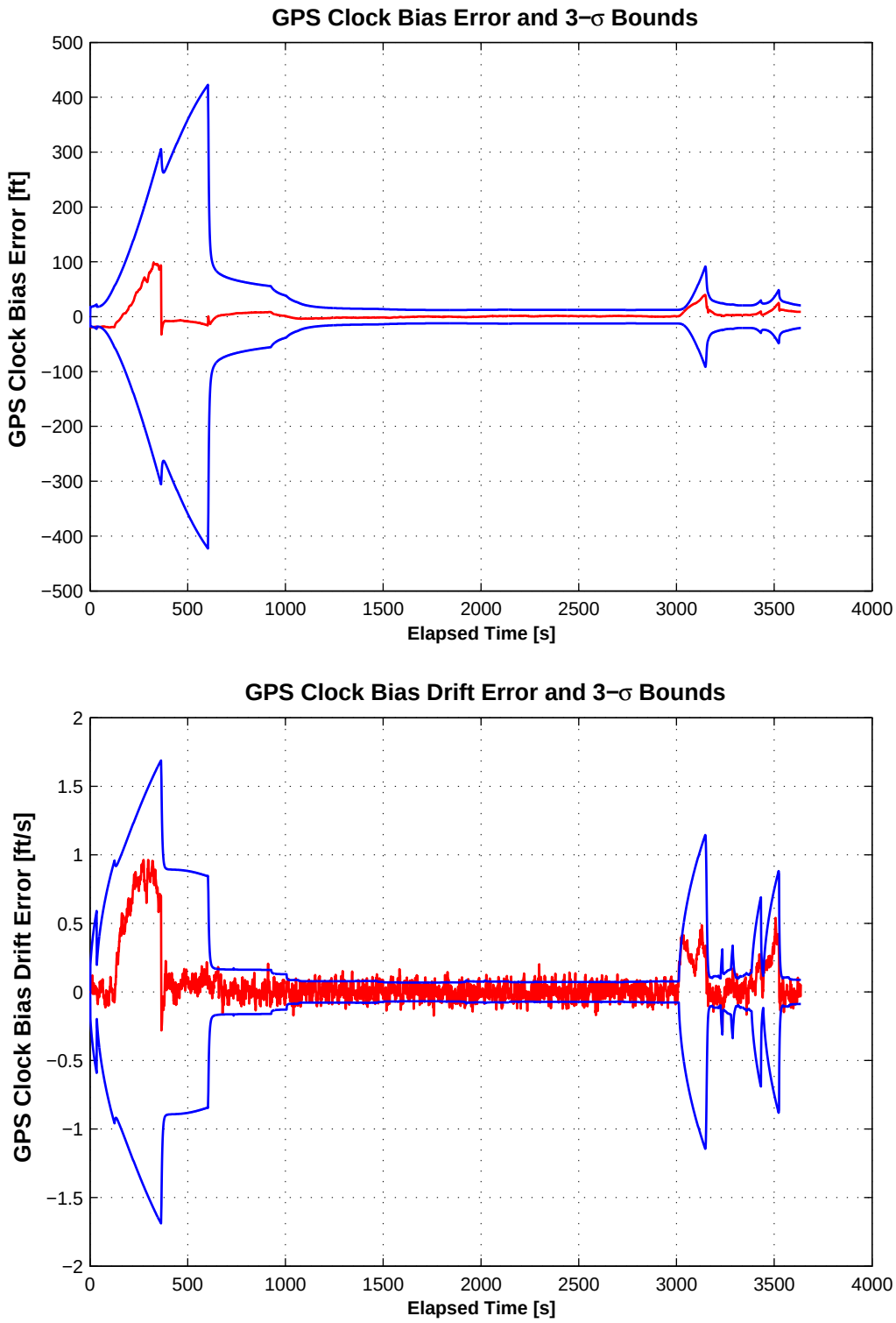

Figure 8. GPS Clock Estimation Performance

However, the implementation is complicated when using the UDU formulation described earlier in this paper. The Orion team has implemented a simple new formulation to allow this, however. It is observed that the effect of underweighting can also be described as simply additive measurement noise. In the Orion EKF, the underweighting correction is simply added to the measurement noise prior to the UDU update.

$$R_{UW} \quad = \quad R + \alpha \mathbf{HPH}^T$$

The result of applying underweighting is a robustness to cases where relatively accurate measurement updates are processed in the presence of large nav errors and large uncertainties. An example is shown in Figure 9.

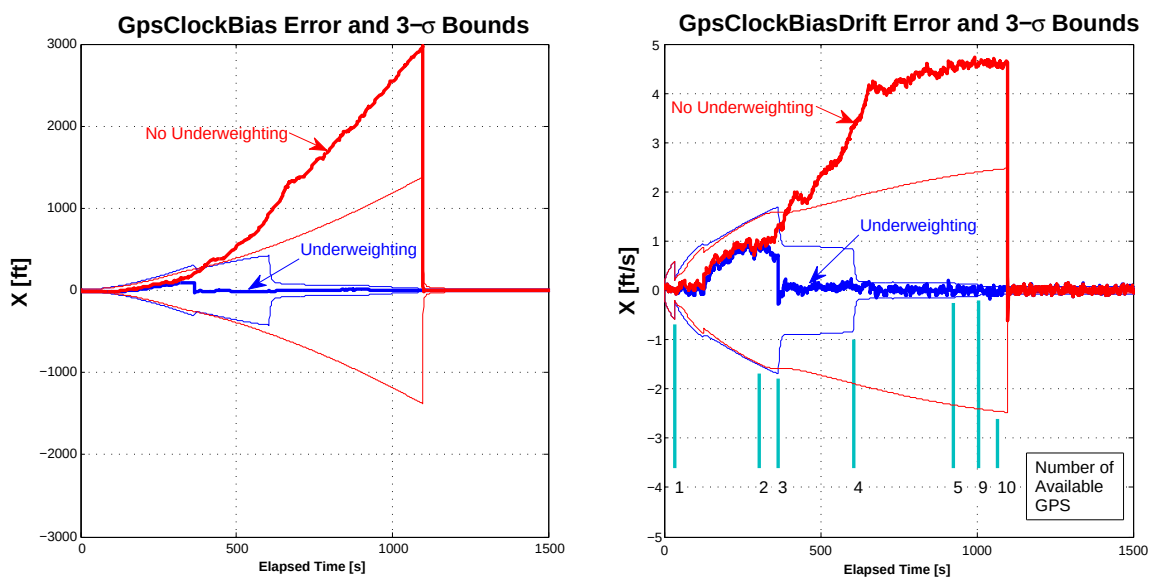

Figure 9. Underweighting Effects on EKF Clock Bias and Drift Estimates

VI. Conclusion

The Orion Absolute Navigation System has matured greatly over the past year. While being rather large in terms of the number of states, many of the states are sensor parameters which are modeled as first-order Gauss-Markov processes. The UDU framework, coupled with the two different Agee-Turner rank-one updates, provides for a computationally efficient and stable methodology, which while requiring a bit more investment in the set-up, results in a larger payoff in the long-term. It has a 'consider covariance' capability designed to allow flexibility for tuning and performance. In addition, it has a measurement underweighting capability to provide a more robust filter architecture.

Acknowledgments

The Orion Absolute Navigation System is a work in progress that has benefited from the efforts of many persons over the course of its multi-year development. The authors wish to acknowledge the valuable contributions of Chad Hanak, Tim Crain, Renato Zanetti, and Robert Gay to its design and implementation.

References

[1]J. A. Klobuchar, "A First-Order, Worldwide, Ionospheric, Time-Delay Algorithm," *Air Force Surveys in Geophysics*, No. 324, 1975.

[2]C. Thornton and G. Bierman, "Gram-Schmidt Algorithms for Covariance Propagation," *IEEE Conference on Decision and Control*, 1975, pp. 489–498.

[3]G. J. Bierman, *Factorization Methods for Discrete Sequential Estimation*. New York: Dover Publications, 2006.

[4]W. Agee and R. Turner, "Triangular Decomposition of a Positive Definite Matrix Plus a Symmetric Dyad with Application to Kalman Filtering," *White Sands Missile Range Tech. Rep. No. 38*, 1972.

[5]N. Carlson, "Fast Triangular Factorization of the Square Root Filter," *AIAA Journal*, Vol. 11, No. 9, 1973, pp. 1259–1265.

[6]S. F. Schmidt, "Application of State-Space Methods to Navigation Problems," *Advances in Control Systems*, Vol. 3, 1966, pp. 293–340.

[7]R. Zanetti, K. DeMars, and R. H. Bishop, "Underweighting Nonlinear Measurements," *Journal of Guidance, Control, and Dynamics*, Vol. 33, September-October 2010, pp. 1670–1675.